Afferent vagal stimulation via gastric electrical stimulation alters sympathetic-vagal balance in domestic pigs – a pilot trial

M. Leitzke[1], S. Schimpf[2], M. Altrock[3], P. Schönknecht[4], S. Bischoff[5], H. Schubert[5], D. Hoyer[6], R. Bauer[7] and S. Olbrich[8]

[1]Helios Clinics, Department of Anaesthesiology, Leisnig, Germany; [2]Dräger Medical GmbH, Lübeck, Germany; [3]MTU Reman Technologies GmbH, Magdeburg, Germany; [4]Leipzig University, Medical faculty, Saxon hospital, Arnsdorf, Germany; [5]University of Jena, Institute for animal testing, experimentation and animal welfare, Jena, Germany; [6]University of Jena, Hans Berger Department of Neurology, Jena, Germany; [7]University of Jena, Institute for molecular cell biology, Jena, Germany; [8]University of Zurich, Department of Psychiatry, Zürich, Switzerland

Received August 28, 2020 – Accepted December 16, 2020

The disturbance of the sympathetic-vagal balance with increasing sympathetic activity and consecutive increase in cytokine release is a major threat in numerous hyperinflammatory syndromes. Therapeutic interventions that modulate the activity in the sympathetic-vagal system are suggested as an effective treatment in these incidences. The purpose of this pilot study was to investigate the effect of electrical stimulation of the gastric wall on sympathetic-vagal balance. German domestic pigs (n=5) were prepared with a modified gastric tube (mGT) for repetitive gastric electrical stimulation (GES). Electrocardiogram was recorded continuously and heart rate variability (HRV) as measure of sympathetic-vagal activity was calculated for three-minute epochs at baseline condition before GES and during GES condition. In comparison to baseline, activity of the autonomic nervous system (ANS) shifted significantly toward increased dominance of vagal activity during GES with a decrease of normalized low frequency (nLF from 58.00 to 25.52) as marker of sympathetic dominance and parallel increase of normalized high frequency (nHF from 41.48 to 74.16) as marker of vagal dominance. During GES, compared to baseline, no difference in heart rate was found. These results indicate that electrical stimulation of the gastric wall may result in shifting the sympathetic-vagal balance toward a parasympathetic predominance.

The autonomic nervous system (ANS) plays an important role in the regulation of respective immune responses to pathological impact (1). The liberation of pro-inflammatory cytokines underlies a very sensitive regulation by ANS afferent sensing and efferent execution (2). Thus, the balance between the sympathetic and the vagal branch of the ANS is indispensable for an appropriately executed immune response (3). Balance disorders of the ANS can be caused by pathological conditions or even may be pathogenic factors themselves (4). Huang et al. (5), for example, found a sympathetic over excitation to be responsible for the autonomic imbalance following endotoxemia (5). Furthermore, Stauss (6, 7) stated an impaired autonomic regulation characterized by low heart rate variability (HRV) to be a marker for negative outcome after myocardial infarction (6) and described its prognostic power

Key words: sympathetic-vagal balance; vagal nerve stimulation; gastric electrical stimulation; heart rate variability; modified gastric tube; hyperinflammatory syndrome

Corresponding Author:
Dr. Marco Leitzke,
Helios Klinik Leisnig, Department of Anaesthesiology,
Colditzer Straße 48, 04703 Leisnig, Germany
Tel.: +49 15771426004/3432182705
Fax: +49 034321 8-133
e-mail: marco.leitzke@gmx.de

0393-974X (2021)

in various different cardiovascular diseases (7). Annane et al. (8) described septic patients with high levels of sympathetic activation and concomitant central autonomic regulatory impairment to be a reasonable explanation for the discrepancy between high sympathetic drive and low HRV (8). In a review, Pavlov et al. (2) pointed out that type 2 diabetes mellitus and the following adverse conditions are also associated with impairment of vagal function (2). Tracey (9) demonstrated the limitation of cytokine release through vagal innervation via the inflammatory reflex (IR) (9). Following pathogen detection in the periphery (10) a vagus-driven afferent signal leads, via central modulation, to an efferent vagal excitation with acetylcholine (Ach) liberation at the spot of impairment. Ach attaches to α7 subunit-characterized nicotinic Ach receptors (α7nAchR) at the surface of cytokine-producing cells, leading to an interruption of cytokine synthesis and release (3). Sepsis and a range of different diseases,, including epilepsy (11–15), depression (12, 13, 16), anxiety (17), Alzheimer's disease (13, 18), dementia (13) vegetative state conditions (19), rheumatoid arthritis (4), inflammatory bowel diseases (20) and potentially chronic heart failure (21), are associated with decreased parasympathetic output and elevated pro-inflammatory serum cytokine levels. The autonomic imbalance therefore catalyzes the pathogenesis of respective disease patterns (22). Elevation of the parasympathetic tone is considered a possible approach (20, 23–26) in the therapeutic management of the aforementioned conditions. Vagal nerve stimulation (VNS) reduces the elevated serum cytokine levels (27), which reveals the enormous therapeutic potential of VNS. Likewise, obesity with its associated comorbidities and metabolic disorders is obviously alleviated by vagal stimulation (28). Recently, Bonaz et al. (29) described the expected high potential of VNS to prevent or ameliorate severe courses of the current pandemic COVID-19 (29), and Staats et al. (30) reported distinct relief of symptoms (fatigue, low appetite, and coughing bouts such as dyspnea and chest pressure/tightness) in two SARS-CoV-2 positive tested patients under the usage of noninvasive vagal nerve stimulation (nVNS) (30).

Numerous investigations presupposed this knowledge to rebalance the ANS via cervical VNS in respective disease patterns and to place an additional tool at the disposal of their treatment (4, 22, 31). In other investigations, the effects of transcutaneous stimulation at the region of the cervical vagus nerve (30, 32) or the auricular branch (33) of the vagus nerve were explored. The results of these trials are promising (34), but to date no investigation (35) has incorporated the IR consisting of an afferent vagal signaling from the spot of impairment, the viscerotopic (36) central sensing and modulation, such as an efferent vagal signal, to deliver Ach for cytokine release control (1). As the cervical vagus nerve contains 20% efferent and 80% afferent fibers (37), cervical VNS causes afferent stimulation of central vagal structures as well as efferent stimulation of vagal innervated organs leading to opposite metabolic effects (38). Furthermore vagal structures are closely connected to sympathetic nerve fibers within the cervical vagus nerve (39) making pure cervical VNS problematic. Thus, cervical VNS in former investigations led to a parallel sympathetic stimulation. This was demonstrated by an enhancement of the low frequency (LF) HRV power (31) and increased firing of stellate ganglion during cervical VNS (40). An anatomic explanation for this effect is given by Seki et al. (39), who found cervical vagal nerves containing sympathetic fibers in every individual (39).

Vagal afferent fibers carry a large amount of information from the gastric wall to the brainstem (41), i.e. the nucleus tractus solitarii (NTS) (41), where this information is transmitted via glutamate related excitation (41) to N-methyl-D-aspartate (NMDA) and non-NMDA neurons of the dorsal vagal motor complex (DVC) to be ultimately converted into accelerated efferent vagal output (41).

Starting from this point, our investigational trial was designed to analyze a stimulation approach, which involves these central structures. In light of the associations mentioned above, the goal of the present pilot study was to investigate whether inductive, i.e. wireless, electrical stimulation of the gastric wall with a modified gastric tube (mGT) can be used for afferent vagal stimulation. We hypothesized that it is possible to enhance the efferent vagal output and suppress

the sympathetic activity, i.e. to shift the sympathetic-vagal balance at the level of HRV towards increased parasympathetic and reduced sympathetic activity via electrical stimulation of the gastric wall without intramural positioning of electrodes.

MATERIALS AND METHODS

Animals

The present study was performed according to the Protection of Animals Act of the Federal Republic of Germany ("Tierschutzgesetz der Bundesrepublik Deutschland") and was approved by the Thuringian State Office for Consumer Protection ("Thüringer Landesamt für Verbraucherschutz, TLV, Reg. No. 02-032/10"). The animals were treated in accordance with the declaration of Helsinki and its guiding principles, with regard to the care and use of animals. Five female German domestic pigs (mean weight: 29.0 kg±1.3 kg) were housed at room temperature before trial preparation. They had access to standard food solution and tap water ad libitum.

Surgical instrumentation

The pigs were sedated by an intramuscular injection with a mixture of ketamine (mean: 0,344 mg/kg ±0.041 mg/kg bodyweight (bw)) and midazolam (mean: 0.067 mg/kg ±0.003 mg/kg bw). An intravenous access (18 Gauge, inner diameter 0.6 mm) was attached to a left-sided ear vein and anesthesia was induced by intravenous administration of fentanyl (mean: 0.003 mg/kg ±0.002 mg/kg bw) and propofol (mean. 0.693 mg/kg ±0.100 mg/kg bw). After positioning and fixation in supine position the animals received orotracheal intubation (spiral tube 5.5 to 6.0 mm inner diameter) and were artificially ventilated to warrant normoxemia and normocapnia. Anesthesia was maintained by sevoflurane (mean alveolar concentration 1.0 to 1.3) in O_2/N_2O (30:70). Proper ventilation was monitored throughout the whole procedure by measurement of arterial oxygen saturation and carbon dioxide concentration in the arterial blood samples. A central venous catheter (PU, 1.4 mm OD) was inserted through a branch of the left external jugular vein to infuse hydroxyethyl starch (HES; 6%; 30ml/h). In addition, an arterial catheter was placed into the left external carotid artery for continuous arterial blood pressure recording and arterial blood sample withdrawal. Electrocardiogram recordings were made from standard limb leads using stainless steel needle electrodes. Catheters and electrode leads were subcutaneously tunneled and led out at the dorsal neck region.

The modified gastric tube (mGT)

We developed a gastric tube based on a percutaneous endoscopic gastrostomy (PEG) tube, providing continuously stable stimulation conditions without mGT impairment from gastric acid. The mucosa adjacent side of

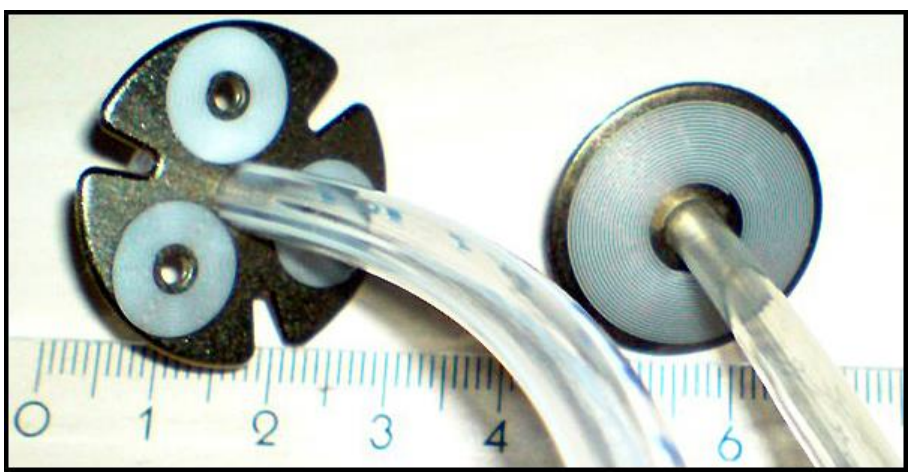

Fig. 1. *Two specimens of the mGT: the mucosa adjacent side of the percutaneous endoscopic gastrostomy (PEG) tube basic plate is metallized with a platinum layer, which is structured by etching to leave a two-dimensional coil. The size of this coil meets with 2 cm diameter the size of the PEG basic plate. In the other specimen three individual coils of 7 mm size have been etched into the platinum layer. For the pilot experiments we used exclusively the greater coils.*

the mGT basic plate was metallized with a two-dimensional platinum coil (Fig. 1) to evoke a signal resulting from an extra corporally placed electromagnet via inductive coupling.

Placement of the mGT

After surgical closure and bandage of the neck incisions, a laparotomy was performed (Fig. 2A). The mGT was placed at the greater curvature in the region of the border between gastric fundus and corpus (Fig. 2B,C) (42) to guarantee optimal stimulation conditions since the density of gastric afferent autonomic neurons is known to be the highest in that region (42). The stomach was sealed by purse-string suture (Fig. 2C). The mGT was driven out through the abdominal wall left beside the incision (Fig. 2D). Surgical closure and sterile bandaging of the abdominal wall were performed. The anesthesia was terminated after the intravenous application of 8 mg phenylbutazone for postoperative analgetic treatment. Extubation was carried out under sufficient spontaneous breathing. After instrumentation, a stabilization period of one hour was given. Subsequently, continuous sedation was established immediately after extubation by α-chloralose infusion (mean 0.14 mg/kg ±0.03 mg/kg bw/min).

Throughout the experiment cardiorespiratory monitoring was performed by regular blood gas check and continuous registration of arterial blood pressure (ABP), respiration movement (RM) and electrocardiogram (ECG). ABP, RM, ECG and body temperature were stored continuously on an external hard drive for off-line data analysis (acquisition software: AtisaPro, Data acquisition & analysis software, GJB Datentechnik GmbH, Langewiesen, Germany; sampling rate 2 kHz).

Pilot experiments

Before starting the original trial, an *ex-vivo* testing of the mGT was performed. Voltage was induced on the mGT through approximately 2.5 cm of porcine muscle tissue. We used a square-wave signal with an amplitude adjusted to 4.5 V as excitation signal. The induction of nerve stimulating voltages through porcine abdominal tissue proved to be feasible and excitation with 4.5 V resulted in induced signal levels with 7 mV amplitudes in the muscular layer.

After a pre-gastric electrical stimulation (pre-GES) condition of at least 15 min, for gastric electrical stimulation (GES) via the mGT a digimess arbitrary wave generator AFG 100 (Grundig electronics) was used. Stimulation (pulse with 330 µs, 30 sec on, 120 sec off) was performed for a stimulation period of at least 10 min. Three animals were stimulated with rectangular and two animals with saw tooth impulses in order to explore whether the waveform of the inductive impulse had an impact on the stimulation effect. Stimulation interval in each animal was carried out with identical intensity parameters (5V; 40Hz). Since vagal afferents originating in the stomach are predominantly unmyelinated C-fibers (41) with a fairly high stimulation threshold responding to short pulse stimulation (43) with a pulse width of 300

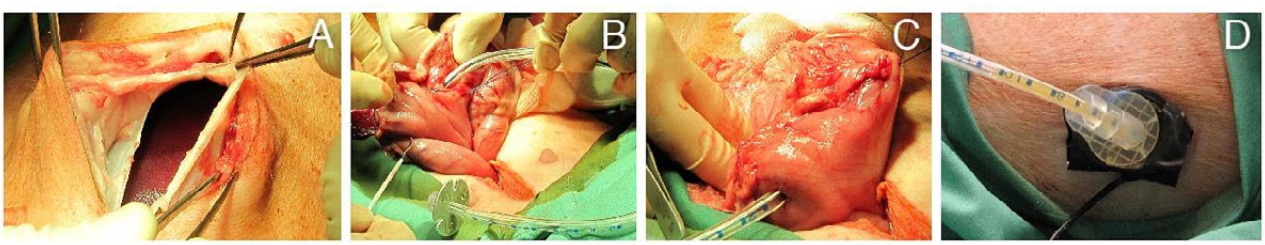

Fig. 2. *Placement of the mGT.* ***A****) laparotomy;* ***B****) placement of the mGT at the greater curvature between gastric fundus and corpus;* ***C****) closure of the stomach by purse string suture;* ***D****) the attached electrical magnet. The electrical magnet envelops the gastric on top of the cutaneous layer of the abdominal wall. An impulse generator is connected to the electrical magnet. This magnet sends a signal (saw tooth or square wave) to the inner coil. This creates inductive impulses in the coil at the basic plate of the mGT. The signal transmission to the inner coil is wireless. The electrical magnet and its alternating field on the abdominal wall induce an electrical voltage on the coil inside the stomach. This voltage excites the structures of the gastric wall outgoing from the mucosal layer.*

μs (44), and with reference to Qin et al. (45) showing neurons in the nucleus tractus solitarii (NTS) are better to stimulate using high amplitude and/or increased pulse width (45), we chose to stimulate with the aforementioned stimulation parameters.

Assessment of cardiac ANS function by HRV analysis

Data from the five pigs was used for statistical analysis, time series included epochs from resting periods (pre-GES) and stimulation periods (GES). After down sampling of ECG raw data from 2000 Hz to 400Hz, done in MATLAB (MATLAB and Statistics Toolbox Release 2012b, The MathWorks, Inc., Natick, Massachusetts, United States.), R-peaks of the ECG- time series were detected automatically using Kubios HRV 2.2 software (http://kubios.uef.fi/). The results were visually inspected for artefacts, epochs with artefacts were excluded. Corrections for erroneous automatic R-peak detections were made if necessary. Electrocardiogram raw data from pre-GES and GES periods were segmented into several artefact-free epochs (ranging from 1-3 epochs for each condition per pig GES or pre-GES), each of 3-minute duration. The first epochs for both conditions and for all pigs were taken from the first three artefact free minutes of recording, consecutive epochs were taken from following artefact free three-minute blocks. Mean duration of pre-GES condition was 45.8 min with SD 25.6 min, GES condition had a mean duration of 20.6 min with SD 22.7 min. A visualization of the timeline from preparation to data assessment can be found in Fig. 3.

Time domain and frequency domain results were computed for each artefact-free three-minute epoch for each pig for the pre-GES and the GES periods. Since for one pig only one epoch of artefact-free data was available, it was discarded from analysis of changes over time. For the 4 other pigs, more than one epoch was available for each of the pre-GES and GES periods. Hence, data was included in the analysis of the impact of time on the time and frequency domain data.

Time domain results included heart rate (HR), root mean square of successive differences (RSSDM) and the proportion of pairs of successive beat-to-beat intervals that differ by more than 50ms (pNN50).

Frequency domain results included total power and

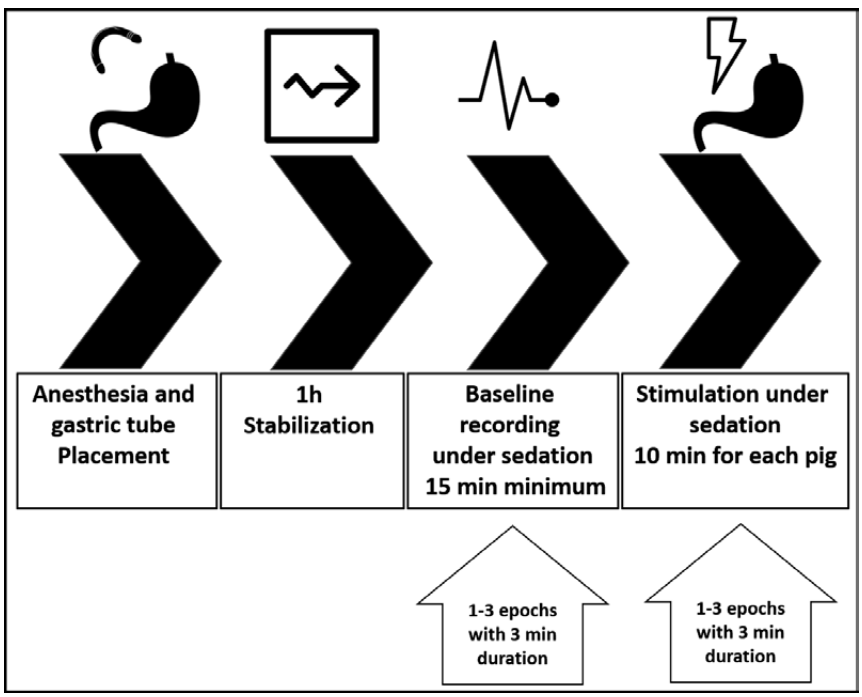

Fig. 3. *Visualisation of the timeline of the study. Visualization of the timeline of preparation and data assessment. Instrumentation was performed under anesthesia, whereas a recovery period from one-hour, such as stimulation and data assessment, was performed under sedation. Since the stimulation period was only 10 minutes, a maximum of 3 three-minute epochs could be included (artefact free).*

the power values of low frequency (LF 0.01-0.13 Hz) and the high frequency (HF 0.13-0.6 Hz), normalized LF (nLF) and the normalized HF (nHF), obtained by fast Fourier transform (FFT), as performed previously (5). Normalized values were computed according to the following formulas (with very low frequency – VLF range from 0-0.01):

$nLF = LF[ms^2]/(\text{total power } [ms^2] - VLF\ [ms^2])$

$nHF = HF[ms^2]/(\text{total power } [ms^2] - VLF\ [ms^2])$

Additionally, we calculated the Poincaré plots with the main parameters of SD 1 (comparable to the parasympathetic driven HF) and SD 2 (comparable to the sympathetic driven LF) for the first epoch of the pre-GES and the GES condition (46).

For the choice of HRV parameters we mainly followed the recommendations of the Task Force of the European Society of Cardiology and the North American Society of Pacing and Electrophysiology (1996) (47). We restricted the time domain measures besides HR to RMSSD and pNN50 since time domain measures are highly intercorrelated. Since the available epochs were restricted to only three-minute segments, RMSSD was especially taken into account since it reflects short-term components of HRV.

For frequency domain analysis, we used a normalized measure to visualize the interaction of both systems. "The representation of LF and HF in normalized units emphasizes the controlled and balanced behavior of the two branches of the autonomic nervous system […and] tends to minimize the effect of the changes in total power on the values of LF and HF components" the (Task Force of the European Society of Cardiology and the North American Society of Pacing and Electrophysiology 1996) (47). However, for reasons of interpretability it is recommended to always also report on the absolute values of HRV power. Furthermore, we decided not to calculate non-linear measures for the presented pilot study due to heterogeneous findings and a lack of clear interpretability.

Statistical analysis

SPSS 20 (IBM Corp. Released 2011. IBM SPSS Statistics, Version 20.0. Armonk, NY: IBM Corp.) was used for statistical analysis. All comparisons between pre-GES and GES condition were made using paired two-sided *T*-tests for the analysis of the first epochs that have been available for all pigs and one-sided for pooling of all epochs of all pigs to test the hypothesis of the direction of change. A p-value < 0.05 was considered significant. For assessment of the effects of time, a repeated measures ANOVA was carried out using the associated HRV parameters of three consecutive time blocks (each of three-minute duration) as repeated measurements. Effect sizes are given in Cohen`s d. A correction for multiple comparison (Bonferroni-correction) was applied to the analysis for test sets from the time domain and frequency

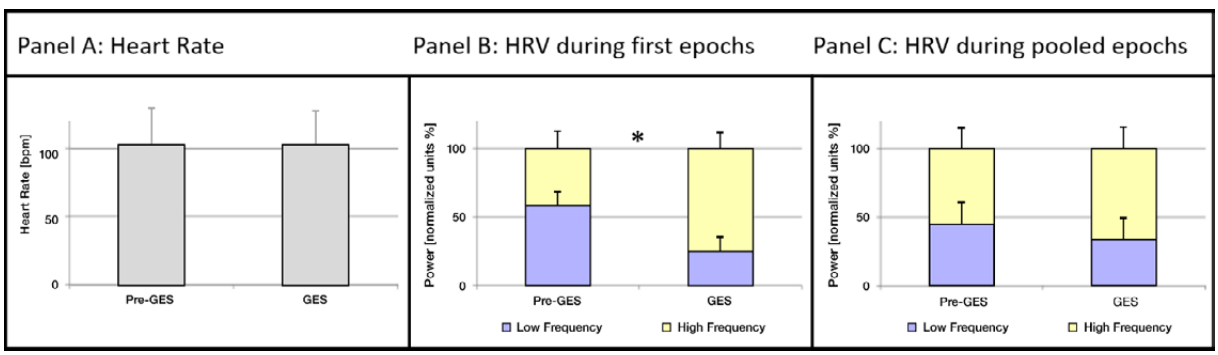

Fig. 4. *HRV parameters: pre-GES vs GES condition. Effect of GES on heart rate (Panel **A**) and HRV (Panel **B**) measures for comparison of the first artefact-free epochs from pre-GES and GES period. While no changes of heart rate occured (Panel A), the data yielded a significant reduction of normalized low-frequency HRV (nLF) and the mathematically corresponding increase of normalized high-frequency power of HRV (nHF) during GES in comparison to pre-GES baseline conditions imediately before stimulation (Panel B). The same pattern can be found for pooling of all epochs, although without statistical significance (Panel **C**), (* - for $p < 0.05$, Bonferroni-corrected for test-sets time domain and frequency domain, whiskers show standard deviation).*

domain. Due to the high inter-correlation, no correction was applied for the number of variables from the test sets (i.e. time domain and frequency domain).

RESULTS

Comparison pre-GES vs GES

Analysis of the first artefact-free three-minute epochs of HRV data during the baseline condition (pre-GES) in comparison to the first artefact-free three-minute epochs during stimulation (GES) revealed no relevant impact on averaged total power or LF/HF ratio (from 1.41 to 0.37, p=0.18 with Cohen`s d=1.52) and a significantly decreased nLF due to stimulation (p=0.04 with Cohen`s d=2.89) with a corresponding increased nHF during stimulation (p=0.04 with Cohen`s d=2.89, Fig. 4, Panel B). No difference was found for the HR (pre-GES 103 b/min, GES 102 b/min; see Fig. 4, Panel A). Likewise no differences were detectable concerning the waveform of the stimulation impulse.

When all available artefact-free epochs of HRV data from the pre-GES and GES periods were pooled (with different amount of epochs from different pigs), again no effect was visible on total power or LF/HF ratio (1.20 to 0.65, not significant with p=0.20, one sided T-test with Cohen`s d=0.84). Again, no differences were found for the HR between pre-GES and GES periods. Also, nLF and nHF showed no-significant differences during GES in comparison to baseline (p=0.16, one sided T-test with Cohen`s d=0.61). Although missing statistical significance in

Table I. *Absolute and normalized time domain and frequency domain values from pre-GES and GES conditions*

	pre-GES (First Epoch)		**GES (First Epoch)**		
	Average	SD	Average	SD	p-Value (t-test two-sided)
HR [bpm]	102.94	26.27	102.60	25.31	1.00
RMSSD [ms]	34.71	17.18	37.16	16.83	1.00
pNN50 [%]	17.65	14.94	16.53	10.84	1.00
Total Power [ms^2]	476.22	500.47	503.60	646.77	1.0
LF [ms^2]	175.95	205.84	93.56	135.01	1.00
HF [ms^2]	138.71	114.51	286.08	316.07	0.64
LF/HF	1.42	0.95	0.37	0.22	0.18
nLF [nu]*	**58.00**	10.57	**25.52**	11.87	**0.04**
nHF [nu]*	**41.48**	10.51	**74.16**	12.08	**0.04**
	pre-GES (All Epochs)		**GES (All Epochs)**		
	Average	SD	Average	SD	p-Value (t-test one-sided)
HR [bpm]	95.94	26.91	97.40	28.29	0.88
RMSSD [ms]	32.15	15.59	34.42	12.05	0.66
pNN50 [%]	16.96	13.03	14.35	8.54	0.56
Total Power [ms^2]	332.09	367.54	411.52	427.72	0.64
LF [ms^2]	106.43	149.80	100.05	92.05	0.90
HF [ms^2]	142.24	136.57	235.49	221.80	0.22
LF/HF	1.12	1.31	0.65	0.66	0.20
nLF [nu]	45.45	21.68	33.69	16.50	0.14
nHF [nu]	54.13	21.66	66.05	16.51	0.14

Table of HRV parameters for pre-GES and GES condition for the first segment of three minutes (top) and all available segments (bottom). (denote p<0.05; Bonferroni-corrected)*

this small group, the direction of change resamples the same reaction found in the analysis for the first available epochs (Fig. 4, Panel C).

Calculating the Poincaré plots revealed that 80% of the pigs showed a decreased SD2/SD1 ratio from pre-GES condition to GES condition (1.1 to 0.6; 1.2 to 1.9; 1.9 to 1.2; 1.2 to 1.0; 1.8 to 1.2) (Fig. 5). This is in line with a decreased sympathetic tone and an increased parasympathetic tone after stimulation.

Repeated measures ANOVA and the impact of time on parameters

To clarify the differences for the "first epoch comparison" of pre-GES *vs* GES periods and "all available epoch" comparisons, a repeated measures ANOVA was carried out with condition (pre-GES vs GES) as group variable and HRV-values of consecutive epochs as time factor (data available for 3 pigs). Heart rate stayed relatively stable during consecutive epochs during pre-GES periods and during GES periods (Fig. 6, Panel A, no group x time interaction). Although LF/HF ratio was higher during pre-GES in comparison to GES epochs, a different picture was seen when analysing nLF and nHF. There was a significant group x time interaction (F=14.03; p=0.03) with a marked decrease of nHF (and consecutive raise of nLF) during GES and the opposite change during baseline condition within the

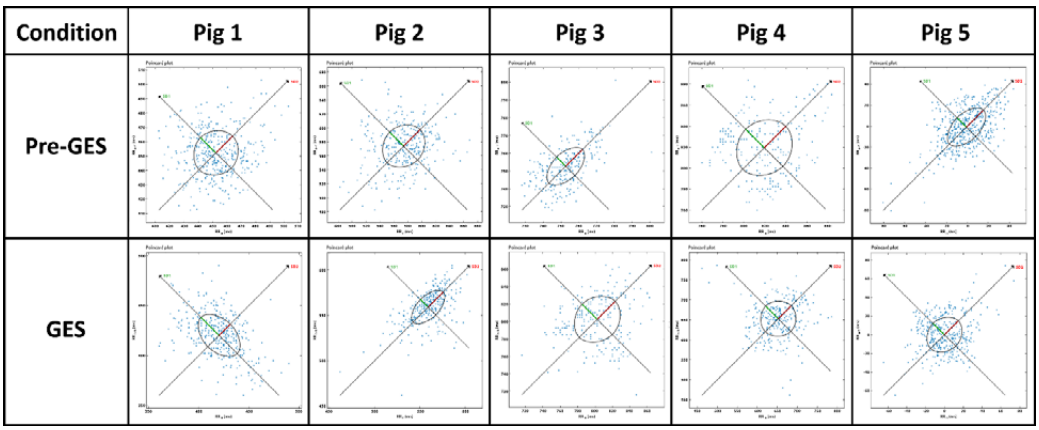

Fig. 5. *Poincaré plots of the pigs for the pre-GES and GES condition. 80% of the pigs (n=5) showed a decreased ratio of the standard deviation 2 (SD2)/standard deviation 1 (SD1) of the plots in line with a shift toward the activity of the parasympathetic branch.*

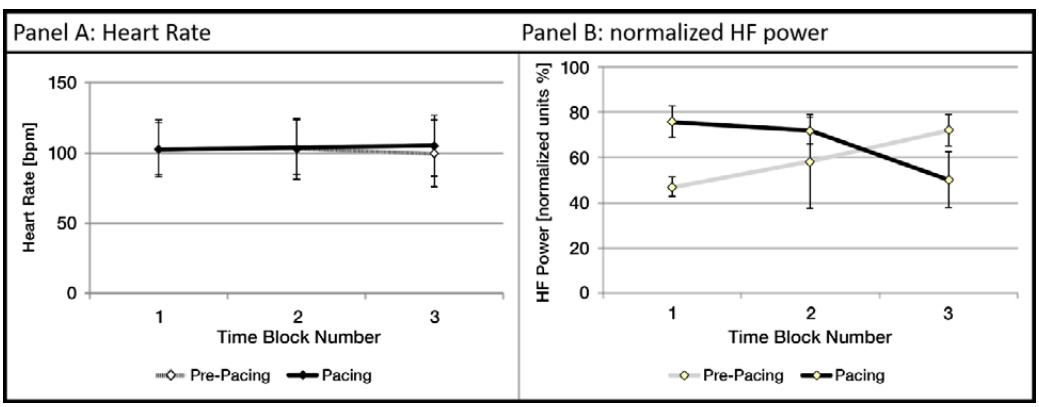

Fig. 6. *Time course of heart rate (Panel **A**) without relevant alterations during consecutive epochs within the pre-GES and GES condition. In contrast, nHF showed a decline during the third epoch of the GES period while during pre-GES epochs an increase occured (Panel **B**). (Whiskers show standard error). The time block numbers are the numbers of the three analyzed consecutive heart rate time series and the corresponding nHF Power values.*

third epoch (Fig. 6, Panel B). Due to the exploratory character of this repeated measures analysis, we did not apply a Bonferroni-correction.

To get a more visual impression of the impact of the stimulation on the HRV parameters and the heart rate itself, we depict a ECG time series before and during GES (Fig. 7). It is clearly visible that while the heart rate did not change, the pattern of RR-interval fluctuations changed dramatically. In the HRV power spectrum a peak within the high frequency reflects this stabilization of RR-interval fluctuations within the stimulation condition in comparison to the baseline.

DISCUSSION

The results of the presented pilot study show that the sympathetic-vagal balance can be shifted toward accelerated activity of the parasympathetic branch of ANS function in pigs by inductive electrical stimulation of the gastric wall. This was found by means of increased normalized high- and respectively decreased normalized low frequency HRV power during stimulation in comparison to baseline condition.

In contrast to former studies for cervical electrical VNS to enhance vagal tone (31, 37, 48, 49), we shifted sympathetic-vagal balance in favor of parasympathetic activity with afferent vagal stimulation via the gastric wall. This stimulation led to relative excitation of central vagal structures resulting in efferent vagal signaling. In comparison to former trials investigating cervical vagal stimulation, the relative enhancement of vagal activity, assessed by analysis of nHF in the current investigation was larger. While in a comparable manner the impairment of relative central sympathetic activity by means of nLF was found to be larger as well (37, 48). In several cervical VNS trials the decrease of sympathetic activity was accompanied by decreasing vagal activity (50) or cervical VNS led to parallel stimulation of the sympathetic ANS branch beside

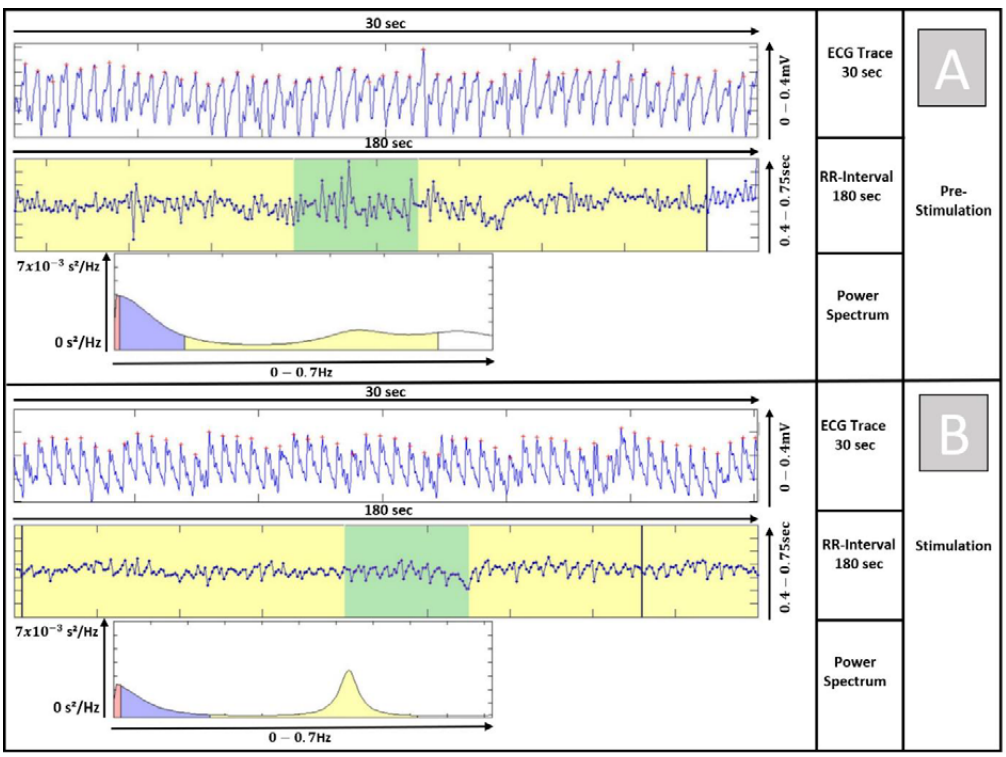

Fig. 7. *Example of ECG traces (30 sec) before (Panel **A**) and during GES (Panel **B**). While the heart rate stayed the same (104bpm in each 3 example), the inter-beat intervals changed as can be visually be assessed within the RR-interval panel for each recording (3 min each). The rhythm stabilized within the high frequency, which also can be seen at the HRV power spectrum where a peak occured within the high frequency range during GES (Panel B) in comparison to pre-GES condition (Panel A).*

increased vagal signaling (31). The current study shows a shift of ANS activity in favor of vagal tone following inductive electrical stimulation of the gastric wall.

The described effects have been identified by evaluation of respective HRV parameters. Since the main difference between former trials and the presented work is that in the current study, using an afferent stimulation approach, we conclude, that these differences in impact on the ANS balance might be attributable to pure afferent stimulation of central vagal structures. It might be hypothesized that this afferent signal is modulated in the NTS (51), representing the principal relay for integrational processing of afferent vagal signaling (52) and converted there, activating dorsal vagal complex (DVC) neurons (51), into efferent vagal pulsation. This central effect could have been evaluated with recording of potentials within the DVC. The impossibility of this measurement due to the study design which focuses on a minimal autonomic interference for evaluating HRV parameters is a clear limitation of our study.

With exclusive afferent stimulation, a stronger efferent autonomic signal promising minor adverse effects seems to be attainable. We think that under clinical conditions the central, and thus integrative part of the IR, is critical for the functionality of the described regulatory loop. Without regarding the current autonomic state, electrical stimulation of the vagal ANS branch results in new autonomic imbalances, which in turn lead to adverse symptoms such as bradycardia (53) up to asystolia (54), bronchoconstriction (38), shortness of breath (12, 14), hoarseness (12, 14, 15), throat pain/dysphagia (12), coughing (12, 14, 15), sleep-related stridor (55) and dizziness (56) or insomnia (12, 56).

However, no significant differences of heart rate (HR), root mean square of successive differences (RSSDM), the proportion of pairs of successive beat-to-beat intervals that differ by more than 50ms (pNN50), absolute HRV power, LF Power or HF power were found in the presented pilot study. Differences were only significant for normalized LF and HF power values, describing a shift of sympathetic-vagal balance rather than changes to one of the ANS branches. Missing significance in non-normalized units might be explained by the quite low number of pigs that increases the variance in the data. The normalization procedure to some degrees counteracts this effect. However, because of missing differences of HR between conditions, an increase of parasympathetic activity at the cost of a decrease of sympathetic power might have led to the differences found in normalized units. Due to the relative low number of pigs in our pilot trial, these effects possibly failed to be significant in the non-normalized absolute values. Although the changes, even of absolute numbers, pointed in this direction, they still fell short of being significant. Trials with more pigs could possibly clarify this issue.

In prior studies (57, 58), heart rate changes were described following efferent VNS, however, they were not observed in the presented study. This initially remarkable fact is attributable to the central rearrangement of viscerotopic (36) afferent vagal signaling (59), which may lead to enhancement of efferent vagal activity without influencing peripheral sympathetic activity.

In the presented study, the effect of vagal stimulation was shown with high significance along the first epoch of the GES interval after pre-GES conditions. Prolonged stimulations (GES) led to a drop of this effect during consecutive epochs, raising the question if the effect was independent of stimulation and would normalize over time by itself. On the other hand-side, it might be explained by the chosen stimulation pattern. Earlier studies detected the stimulation frequency to be the most critical point regarding the stimulation parameters (60–62). Chen et al. (61) pointed out that a presynaptic mechanism contributes to depression of autonomic signal transmission in NTS in frequencies above 0.1 Hz (61). Likewise, Lehrer et Gevirtz (62) showed the resonance frequency of the vagal system to be 0.1 Hz indicated by the HF power of HRV (62), thus, the chosen stimulation frequency was most likely much too high and perhaps could have caused the signal transmitting depression in NTS mentioned above as well as exhaustion of the peripheral signal transmitting structures as defined by a local cholinergic deficit, which limits the excitability of

the stimulated circuit. Nevertheless, the number of included animals within our pilot trial was too small to draw general conclusions and further studies with larger N should be used to replicate this finding. A larger study is underway.

The number of indicators for evaluation of autonomic balance is very low. Some authors investigated the skin conductivity level (SCL) (63) describing solely the sympathetic activity of the ANS (63), which was never used for the measurement of ANS balance in animals. Rocchetti et al. (64) compared the concentration of autonomic agonists (Ach) in sinoatrial myocytes with the baroreflex sensitivity (BRS) and time domain HRV parameters (64) and did find no linear correlation. Zaza and Lombardi (65) referring to the results of Rochetti et al. (64) pointed out that normalized frequency domain indexes of HRV for their HR-independency appear to be appropriate indexes for analyzing sympathetic-vagal balance (65). Furthermore they doubt the validity of the BRS describing ANS balance for its lack of concomitant changes in LF/HF ratio and the high affectability by mean heart rate (65). Chang et al. (66) could show that functional magnetic resonance imaging (fMRI) changes in several brain areas correlate with changes in frequency domain HRV parameters (66). Taking into consideration the issues mentioned above, we performed our observation of the ANS balance analyzing the given HRV parameters.

The evaluation of the ANS tone under sedation remains debatable, but due to animal safety and welfare sedation for GES was unavoidable. The drug α-chloralose is widely used as an anesthetic in studies of the cerebral vascular system because of its presumed minimal depression of autonomic function (67). Different authors pointed out that α-chloralose only minimally affects cardiorespiratory function and preserves autonomic reflex stability remarkably well (68, 69).

We conclude that inductive GES via a mGT appears to be a promising approach to alter sympathetic-vagal balance by enlarging vagal and depressing sympathetic activity relatively in order to prevent consecutive pathologies due to a compromised vagal system. Further investigations of afferent vagal stimulation must explore the optimal stimulation pattern, highlighting the stimulation frequency such as energy and wavelength to maximize the effects on ANS function and balance. Likewise, effects of a longer period of vagal stimulation via the gastric wall must be examined in following trials to appraise the potential of afferent vagal stimulation for a clinical setting.

ACKNOWLEDGEMENTS

We thank the employees at the Institute for Animal Testing, Experimentation and Animal Welfare of Jena University for their careful handling and treatment of the animals and for analyzing the blood samples. We thank Creed Weiler and Ivan Milencovic for critically reading the manuscript. ML thanks his principal consultant Jan Jacob Meyer for providing time to write the manuscript. Not least, thanks to Frank Jabin for his creative work on the figures.

DISCLOSURES: Marco Leitzke, Stefan Schimpf and Martin Altrock are inventors on one patent application (DE 10 2010 055 792.7 Number) related to gastric electrical stimulation, but do not receive any proceeds related to this patent, so that no financial or non-financial compenting interests are given. Harald Schubert, Sabine Bischoff, Dirk Hoyer, Peter Schönknecht and Sebastian Olbrich report no financial and no non-financial conflict of interest. No funding was obtained.

REFERENCES

1. Tracey KJ. Physiology and immunology of the cholinergic antiinflammatory pathway. J Clin Invest 2007; 117(2):289–96.
2. Pavlov VA, Tracey KJ. The vagus nerve and the inflammatory reflex—linking immunity and metabolism. Nat Rev Endocrinol 2012; 8(12):743–54.
3. Wang H, Yu M, Ochani M, et al. Nicotinic acetylcholine receptor alpha7 subunit is an essential regulator of inflammation. Nature. 2003; 421(6921):384–8.
4. Koopman FA, Tang MW, Vermeij J, et al. Autonomic dysfunction precedes development of rheumatoid arthritis: a prospective cohort study. EBioMedicine

2016; 6:231–7.
5. Huang J, Wang Y, Jiang D, Zhou J, Huang X. The sympathetic-vagal balance against endotoxemia. J Neural Transm 2010; 117(6):729–35.
6. Stauss HM. Heart rate variability. Am J Physiol - Regul Integr Comp Physiol 2003; 285(5):R927–31.
7. Stauss HM. Heart rate variability: just a surrogate for mean heart rate? Hypertension 2014; 64(6):1184–6.
8. Annane D, Trabold F, Sharshar T, Jarrin I, Blanc AS, Raphael JC, Gajdos P. Inappropriate sympathetic activation at onset of septic shock: a spectral analysis approach. Am J Respir Crit Care Med 1999; 160(2):458–65.
9. Tracey KJ. The inflammatory reflex. Nature 2002; 420(6917):853–9.
10. Andersson J. The inflammatory reflex--introduction. J Intern Med 2005; 257(2):122–5.
11. Romigi A, Albanese M, Placidi F, et al. Heart rate variability in untreated newly diagnosed temporal lobe epilepsy: Evidence for ictal sympathetic dysregulation. Epilepsia. 2016; 57(3):418–26.
12. Ohemeng KK, Parham K. Vagal nerve stimulation: indications, implantation, and outcomes. Otolaryngol Clin North Am 2020; 53(1):127–43.
13. Broncel A, Bocian R, Kłos-Wojtczak P, Kulbat-Warycha K, Konopacki J. Vagal nerve stimulation as a promising tool in the improvement of cognitive disorders. Brain Res Bull 2020; 155:37–47.
14. Ellrich J. Transcutaneous auricular vagus nerve stimulation. J Clin Neurophysiol Off Publ Am Electroencephalogr Soc 2019; 36(6):437–42.
15. González HFJ, Yengo-Kahn A, Englot DJ. Vagus nerve stimulation for the treatment of epilepsy. Neurosurg Clin N Am 2019; 30(2):219–30.
16. Akar SA, Kara S, Bilgiç V. Investigation of heart rate variability in major depression patients using wavelet packet transform. Psychiatry Res 2016; 238:326–32.
17. Alvares GA, Quintana DS, Hickie IB, Guastella AJ. Autonomic nervous system dysfunction in psychiatric disorders and the impact of psychotropic medications: a systematic review and meta-analysis. J Psychiatry Neurosci 2016; 41(2):89–104.
18. Struhal W, Mahringer C, Lahrmann H, Mörtl C, Buhl P, Huemer M, Ransmayr G. Heart rate spectra confirm the presence of autonomic dysfunction in dementia patients. J Alzheimers Dis JAD. 2016; 54(2):657-67
19. Corazzol M, Lio G, Lefevre A, et al. Restoring consciousness with vagus nerve stimulation. Curr Biol. 2017; 27(18):R994–6.
20. Bonaz B, Sinniger V, Hoffmann D, et al. Chronic vagus nerve stimulation in Crohn's disease: a 6-month follow-up pilot study. Neurogastroenterol 2016; 28(6):948–53.
21. Gold MR, Van Veldhuisen DJ, Hauptman PJ, et al. Vagus nerve stimulation for the treatment of heart failure. J Am Coll Cardiol 2016; 68(2):149–58.
22. Coruzzi P, Castiglioni P, Parati G, et al. Autonomic cardiovascular regulation in quiescent ulcerative colitis and Crohn's disease. Eur J Clin Invest 2007; 37(12):964–70.
23. Tsai J-D, Chang Y-C, Lin L-C, Hung K-L. The neuropsychological outcome of pediatric patients with refractory epilepsy treated with VNS — A 24-month follow-up in Taiwan. Epilepsy Behav 2016; 56:95–8.
24. Milev RV, Giacobbe P, Kennedy SH, et al. Canadian network for mood and anxiety treatments (CANMAT) 2016 clinical guidelines for the management of adults with major depressive disorder: section 4. neurostimulation treatments. Can J Psychiatry 2016; 61(9):561–75.
25. Merrill CA, Jonsson MAG, Minthon L, et al. Vagus nerve stimulation in patients with Alzheimer's disease: Additional follow-up results of a pilot study through 1 year. J Clin Psychiatry 2006; 67(8):1171–8.
26. Nishizaki A, Sakamoto K, Saku K, et al. Optimal titration is important to maximize the beneficial effects of vagal nerve stimulation in chronic heart failure. J Card Fail 2016; 22(8):631–8.
27. Borovikova LV, Ivanova S, Zhang M, et al. Vagus nerve stimulation attenuates the systemic inflammatory response to endotoxin Nature. 2000; 405(6785):458–62.
28. Samniang B, Shinlapawittayatorn K, Chunchai T, et al. Vagus nerve stimulation improves cardiac function by preventing mitochondrial dysfunction in obese-insulin resistant rats. Sci Rep 2016; 6:19749.
29. Bonaz B, Sinniger V, Pellissier S. Targeting the cholinergic anti-inflammatory pathway with vagus nerve stimulation in patients with Covid-19? Bioelectron Med 2020; 6(1):1-7.

30. Staats P, Giannakopoulos G, Blake J, Liebler E, Levy RM. The use of non-invasive vagus nerve stimulation to treat respiratory symptoms associated with COVID-19: a theoretical hypothesis and early clinical experience. Neuromodulation Technol Neural Interface 2020; 23:784-8.
31. Martlé V, Bavegems V, Van Ham L, et al. Evaluation of heart rate variability in dogs during standard and microburst vagus nerve stimulation: a pilot study. Vet J 2014; 202(3):651–3.
32. Xu F, Tan Y, Huang Z, Zhang N, Xu Y, Yin J. Ameliorating effect of transcutaneous electroacupuncture on impaired gastric accommodation in patients with postprandial distress syndrome-predominant functional dyspepsia: a pilot study. Evid Based Complement Alternat Med 2015; 2015:1–7.
33. Van Leusden JWR, Sellaro R, Colzato LS. Transcutaneous Vagal Nerve Stimulation (tVNS): a new neuromodulation tool in healthy humans? Front Psychol 2015 Feb; 6:102.
34. Levine YA, Koopman FA, Faltys M, et al. Neurostimulation of the cholinergic anti-inflammatory pathway ameliorates disease in rat collagen-induced arthritis. PLoS ONE. 2014; 9(8):e104530.
35. Guiraud D, Andreu D, Bonnet S, et al. Vagus nerve stimulation: state of the art of stimulation and recording strategies to address autonomic function neuromodulation. J Neural Eng 2016; 13(4):041002.
36. McDougall SJ, Peters JH, Andresen MC. Convergence of cranial visceral afferents within the solitary tract nucleus. J Neurosci 2009; 29(41):12886–95.
37. Jansen K, Vandeput S, Milosevic M, et al. Autonomic effects of refractory epilepsy on heart rate variability in children: influence of intermittent vagus nerve stimulation. Dev Med Child Neurol 2011; 53(12):1143–9.
38. Meyers EE, Kronemberger A, Lira V, Rahmouni K, Stauss HM. Contrasting effects of afferent and efferent vagal nerve stimulation on insulin secretion and blood glucose regulation. Physiol Rep 2016; 4(4):e12718.
39. Seki A, Green HR, Lee TD, et al. Sympathetic nerve fibers in human cervical and thoracic vagus nerves. Heart Rhythm Off J Heart Rhythm Soc 2014; 11(8):1411–7.
40. Rhee K-S, Hsueh C-H, Hellyer JA, et al. Cervical vagal nerve stimulation activates the stellate ganglion in ambulatory dogs. Korean Circ J 2015; 45(2):149-157.
41. Kentish SJ, Page AJ. Plasticity of gastro-intestinal vagal afferent endings. Physiol Behav 2014; 136:170–8.
42. Komuro T. Structure and organization of interstitial cells of Cajal in the gastrointestinal tract. J Physiol 2006; 576(3):653–8.
43. Liu J, Qiao X, Chen JDZ. Vagal afferent is involved in short-pulse gastric electrical stimulation in rats. Dig Dis Sci 2004; 49(5):729–37.
44. Castoro MA, Yoo PB, Hincapie JG, Hamann JJ, Ruble SB, Wolf PD, Grill WM. Excitation properties of the right cervical vagus nerve in adult dogs. Exp Neurol 2011; 227(1):62–8.
45. Qin C, Sun Y, Chen JDZ, Foreman RD. Gastric electrical stimulation modulates neuronal activity in nucleus tractus solitarii in rats. Auton Neurosci 2005; 119(1):1–8.
46. Hsu C-H, Tsai M-Y, Huang G-S, et al. Poincaré plot indexes of heart rate variability detect dynamic autonomic modulation during general anesthesia induction. Acta Anaesthesiol Taiwan 2012; 50(1):12–8.
47. Task Force of the European Society of Cardiology and the North American Society of Pacing and Electrophysiology. Heart rate variability. Standards of measurement, physiological interpretation, and clinical use. Eur Heart J 1996;17(3):354–81.
48. Zhang Y, Popovic ZB, Bibevski S, Fakhry I, Sica DA, Van Wagoner DR, Mazgalev TN. Chronic vagus nerve stimulation improves autonomic control and attenuates systemic inflammation and heart failure progression in a canine high-rate pacing model. Circ Heart Fail 2009; 2(6):692–9.
49. Verrier RL, Nearing BD, Olin B, Boon P, Schachter SC. Baseline elevation and reduction in cardiac electrical instability assessed by quantitative T-wave alternans in patients with drug-resistant epilepsy treated with vagus nerve stimulation in the AspireSR E-36 trial. Epilepsy Behav 2016; 62:85–9.
50. Schomer AC, Nearing BD, Schachter SC, Verrier RL. Vagus nerve stimulation reduces cardiac electrical instability assessed by quantitative T-wave alternans analysis in patients with drug-resistant focal epilepsy. Epilepsia 2014; 55(12):1996–2002.
51. Travagli RA, Hermann GE, Browning KN, Rogers

RC. Brainstem circuits regulating gastric function. Annu Rev Physiol. 2006 Jan;68(1):279–305.
52. Smith DV, Uteshev VV. Heterogeneity of nicotinic acetylcholine receptor expression in the caudal nucleus of the solitary tract. Neuropharmacology. 2008 Feb;54(2):445–53.
53. Asconapé JJ, Moore DD, Zipes DP, Hartman LM, Duffell WH. Bradycardia and asystole with the use of vagus nerve stimulation for the treatment of epilepsy: a rare complication of intraoperative device testing. Epilepsia 1999; 40(10):1452–4.
54. Tatum WOT, Moore DB, Stecker MM, et al. Ventricular asystole during vagus nerve stimulation for epilepsy in humans. Neurology 1999; 52(6):1267–1267.
55. Louis EKS, Faber K. Reversible sleep-related stridor during vagus nerve stimulation. Epileptic Disord 2010; 12(1):76–80.
56. Sackeim H. Vagus Nerve Stimulation (VNS™) for Treatment-resistant depression efficacy, side effects, and predictors of outcome. Neuropsychopharmacology. 2001; 25(5):713–28.
57. Agarwal R, Mokelke E, Ruble SB, Stolen CM. Vagal nerve stimulation evoked heart rate changes and protection from cardiac remodeling. J Cardiovasc Transl Res. 2016; 9(1):67–76.
58. Yamakawa K, So EL, Rajendran PS, et al. Electrophysiological effects of right and left vagal nerve stimulation on the ventricular myocardium. AJP Heart Circ Physiol 2014; 307(5):H722–31.
59. Niijima A. The afferent discharges from sensors for interleukin 1 beta in the hepatoportal system in the anesthetized rat. J Auton Nerv Syst 1996 Dec; 61(3):287–91.
60. Le Blanc-Louvry I, Guerre F, Songné B, Ducrotté P. Gastric stimulation: influence of electrical parameters on gastric emptying in control and diabetic rats. BMC Surg 2002; 2(1):5.
61. Chen C-Y, Horowitz JM, Bonham AC. A presynaptic mechanism contributes to depression of autonomic signal transmission in NTS. Am J Physiol-Heart Circ Physiol 1999; 277(4):H1350–60.
62. Lehrer PM, Gevirtz R. Heart rate variability biofeedback: how and why does it work? Front Psychol 2014; 5:756
63. Counotte J, Pot-Kolder R, van Roon AM, Hoskam O, van der Gaag M, Veling W. High psychosis liability is associated with altered autonomic balance during exposure to Virtual Reality social stressors. Schizophr Res 2017; 184:14–20.
64. Rocchetti M, Malfatto G, Lombardi F, Zaza A. Role of the input/output relation of sinoatrial myocytes in cholinergic modulation of heart rate variability. J Cardiovasc Electrophysiol 2000; 11(5):522–30.
65. Zaza A, Lombardi F. Autonomic indexes based on the analysis of heart rate variability: a view from the sinus node. Cardiovasc Res 2001; 50(3):434–42.
66. Chang C, Metzger CD, Glover GH, Duyn JH, Heinze H-J, Walter M. Association between heart rate variability and fluctuations in resting-state functional connectivity. NeuroImage 2013; 68:93–104.
67. Luckl J, Keating J, Greenberg JH. Alpha-chloralose is a suitable anesthetic for chronic focal cerebral ischemia studies in the rat: A comparative study. Brain Res 2008; 1191:157–67.
68. Arfors K-E, Arturson G, Malmberg P. Effect of prolonged chloralose anesthesia on acid-base balance and cardiovascular functions in dogs. Acta Physiol Scand 1971; 81(1):47–53.
69. Lindauer U, Villringer A, Dirnagl U. Characterization of CBF response to somatosensory stimulation: model and influence of anesthetics. Am J Physiol. 1993; 264(4 Pt 2):H1223-1228.